Physical Structure, Characteristics, and Applications of Monolithic Bidirectional Switches: A Comprehensive Review

Guangyu Wang, *Graduate Student Member, IEEE*, Huiqing Wen, *Senior Member, IEEE*, Wen Liu, *Senior Member, IEEE*, and Fan Li, *Member, IEEE*

***Abstract*—Bidirectional switches (BiSs) own excellent characteristics, allowing bidirectional current flow during conduction period and withstanding bidirectional voltage when turned OFF. However, traditional BiSs are typically implemented by the association of unidirectional discrete devices, such as the series and antiparallel connection of two active devices and two diodes, which exhibit relatively large device size and conduction losses due to the ON-state voltage offset. With the popularity of wide band-gap (WBG) semiconductor materials such as SiC and GaN, there is an urgent need to design BiSs with lower on-state voltage drop, smaller conduction losses, smaller device size, and consequently higher power density. Therefore, by integrating several power transistors into a single chip, monolithic bidirectional switches (MBSs) based on WBG semiconductor materials can achieve this goal very well, exhibiting high-frequency and fast switching while reducing parasitic inductance and conduction resistance. This article provides a comprehensive review of MBSs from the perspectives of materials, physical structures, characteristics, and applications for the first time, which is helpful for the in-depth optimization and future large-scale promotion of MBSs.**

***Index Terms*—GaN, matrix converter, monolithic bidirectional switch, review, SiC.**

I. Introduction

THE rapid development of technologies such as electric vehicles, sustainable energy, smart grids, and zero carbon buildings has increasingly raised the demand for power electronic topologies and semiconductor devices. Power electronic topologies such as matrix converters [1], current source converters [2], and multilevel T-type inverters [3] have become very popular and been widely applied in industry. This places high demands on power semiconductor devices with bidirectional current flow capability in the ON state and bidirectional voltage blocking capability in the OFF state. For instance, matrix converters have been widely regarded as the most efficient topology due to the direct ac–ac single-stage power conversion, where bidirectional switches (BiSs) are commonly regarded the most critical components in matrix converters [1].

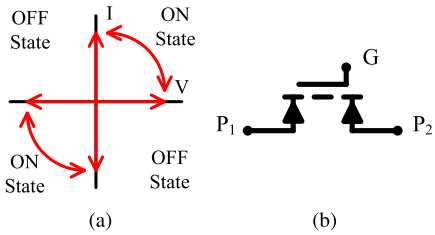

Fig. 1. Schematic diagram of BiSs: (a) Working quadrants. (b) Electrical symbol.

BiSs are also referred to as bilateral switches, ac switches, or four-quadrant switches in some literature [4]. Since their official introduction in 1998, BiSs have received widespread attention due to their unique characteristics such as bidirectional current flow capability in conducting state and bidirectional withstand voltage capability in the OFF state. As shown in Fig. 1(a), BiSs can operate in the OFF state, which is the second and fourth quadrant, to block the voltage between the two polarities. It can also operate in the ON state, which is the first and third quadrants, to conduct the current in any direction based on the actual control signal. BiSs usually have one or two gates, denoted by G, and two power ports, P_1 and P_2, embedded in the main power circuit. The electrical symbol of BiSs is shown in Fig. 1(b).

Although BiSs are the critical components that make up topology such as matrix converters and multilevel T-type inverters, there are still very few commercially available BiSs in the power electronics market. So far, the function of BiSs is usually realized by three methods: 1) unidirectional discrete device combination (UDDC) method; 2) voltage-controlled-devices based monolithic integration (VCD-MI) method; and 3) current-controlled-devices based monolithic integration (CCD-MI) method.

Received 20 November 2024; revised 13 January 2025; accepted 12 February 2025. Date of publication 18 February 2025; date of current version 14 April 2025. This work was supported in part by the National Natural Science Foundation of China under Grant 52177195, in part by the Jiangsu Science and Technology Programme under Grant BK20220029, in part by the Suzhou Prospective Application programme under Grant SYG202016, and in part by the Suzhou Industrial Park High Quality Innovation Platform Construction Project, and Suzhou Smart Energy Technology Key Laboratory Project under Grant SKLSET2309 and Grant SKLSET2302. Recommended for publication by Associate Editor J. Lam. *(Corresponding author: Huiqing Wen.)*

Guangyu Wang and Fan Li are with the Department of Electrical Engineering and Electronics, University of Liverpool, L69 3BX Liverpool, U.K., and also with the Department of Electrical and Electronic Engineering, Xi'an Jiaotong-Liverpool University, Suzhou 215123, China (e-mail: Guangyu.wang19@student.xjtlu.edu.cn; Fan.li19@alumni.xjtlu.edu.cn).

Huiqing Wen and Wen Liu are with the Department of Electrical and Electronic Engineering, Xi'an Jiaotong-Liverpool University, Suzhou 215123, China (e-mail: Huiqing.Wen@xjtlu.edu.cn; Wen.Liu@xjtlu.edu.cn).

Color versions of one or more figures in this article are available at https://doi.org/10.1109/TPEL.2025.3543635.

Digital Object Identifier 10.1109/TPEL.2025.3543635

Early BiSs typically adopt the UDDC method due to limitations in chip manufacturing technology and material performance [5]. With the association of unidirectional discrete devices, such as the series and anti-parallel connection of two active devices and two diodes, UDDC-based BiSs exhibit relatively large device size and conduction losses due to the ON-state voltage offset. For instance, as a feasible method to achieve BiSs functionality, the reverse series connection of two field-effect transformers (FETs) will increase the total on-resistance by two times compared to a single device. Therefore, two branches with internal devices connected in reverse series are usually arranged in parallel to reduce the total conduction resistance, exhibiting the factor-of-four penalty in terms of the chip area usage. The limitation of UDDC-based BiSs, such as large device size and conduction losses due to the ON-state voltage offset, has become one of the main obstacles in exploring the full potential of advanced topologies such as matrix converters and T-type inverters, demanding high power integration to achieve high-frequency fast switching while reducing parasitic inductance and conduction resistance.

By integrating several power transistors into a single chip, monolithic bidirectional switches (MBSs) are capable of providing smaller chip size, lower conduction resistance, and higher switching frequency compared with UDDC-based BiSs. Therefore, highly integrated MBSs have gradually entered people's vision in recent years, including both VCD-MI based MBSs [6], [7], [8] and CCD-MI based MBSs [9], [10], [11].

Regarding VCD-MI based MBSs, [6] discussed a vertical bidirectional MOS-thyristor device with a new triggering mode. In [7], the fabrication process of MBSs with MOS-controlled emitter structures was presented. The designed MBSs with a real punch-through structure was capable of achieving high blocking voltage and low conduction losses, which are close to the limit of silicon material. In [8], a bidirectional IGBT was designed using the double side photo-lithography technique. However, the designed bidirectional IGBT exhibited an asymmetrical electrical characteristic in terms of the I-V curve in the forward and reverse conducting states. Regarding CCD-MI based MBSs, [9] and [10] discussed monolithic current bidirectional bipolar transistors, which exhibits relative complicated control circuit and realization procedure. In [11], an improved scheme called Bipolar AC (Bipac) was proposed to reduce the fabrication cost and simplify the control circuit design. However, this design was dedicated to specific mains applications with low load current. Furthermore, all these prior studies for MBSs originate from the integrated process of silicon materials, so device characteristics are significantly limited by the inherent properties of silicon material.

With the popularity of wide band-gap (WBG) semiconductor materials such as SiC and GaN, there is an urgent need to design MBSs with lower ON-state voltage drop, smaller conduction losses, smaller device size, and consequently higher power density. Therefore, MBSs based on WBG semiconductor materials can achieve this goal very well, exhibiting higher switching frequency while reducing parasitic inductance and conduction resistance [9], [12]. For instance, monolithically integrated bidirectional GaN high-electron-mobility transistors (HEMTs) can reduce the ON-resistance (R_{on}) by up to 50% compared to discrete bidirectional switches through a common drift region design for blocking both voltage polarities [12], [13].

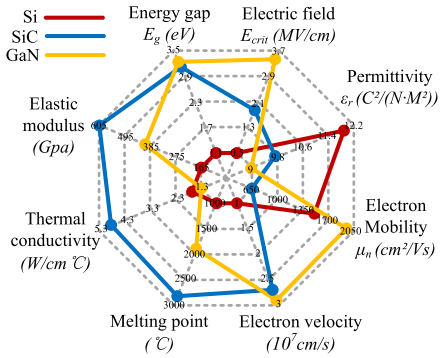

Fig. 2. Comparison of three semiconductor materials for MBSs.

Before designing power converters with MBSs, it is natural and necessary to understand the main characteristics and challenges brought by these devices and their power integrated techniques, especially the emerging WBG devices. Although several review and survey articles have been published on characteristics and applications of WBG devices, including commercial GaN power devices, gate driver design, loss distribution, reliability, pulse test techniques, power integration and typical applications, there is a lack of a comprehensive review of WBG-based MBSs. In order to fill this gap, this article provides a comprehensive comparison of various MBSs from the perspectives of materials, physical structure, characteristics, and applications for the first time, which is helpful for the in-depth optimization and future large-scale promotion of MBSs.

II. Semiconductor Materials for MBSs

WBG devices are becoming increasingly popular due to their superior performance. Among various WBG materials, SiC and GaN devices exhibit excellent material properties, particularly high blocking voltage capability, high-temperature operation capability, and high switching frequency. Fig. 2 shows the comparison among SiC, GaN, and Si in terms of key material properties [14]. Among them, the energy gap and electric field can demonstrate the potential of materials under harsh working conditions such as high voltage. The dielectric constant, electric mobility, and electric velocity can demonstrate the high-frequency performance of materials. The melting point, thermal conductivity, and elastic modulus can demonstrate the working performance of materials in harsh environments such as high temperatures.

Due to the high critical field of WBG material shown in Fig. 2, the drift region of WBG power switches is usually narrower than that of Si power switches with the same rated voltage. That is to say, under the same breakdown voltage requirements, the chip size of switching devices made of WBG material is smaller than that of Si devices, and the conduction resistance in the drift region is smaller [12]. Power semiconductor devices made of WBG materials can achieve lower power losses and higher switching frequencies. However, the fast switching action and high-frequency operation of WBG devices have brought

new challenges to device applications and safe and reliable operation, with electromagnetic interference being one of the main challenges [15].

The production cost of MBSs based on silicon materials is low, and their manufacturing process is relatively mature. The combination and sharing of partial structures based on existing silicon power devices can easily design MBSs. However, due to the inherent properties of the material, MBSs based on silicon material do not exhibit excellent performance under high-voltage and high-frequency conditions. Compared with MBSs based on WBG materials, it prefers silicon-based MBSs with a rated voltage below 600 V because the price is relatively low and the conduction loss is comparable.

The excellent material characteristics of SiC enabled SiC devices to have lower switching losses and better switching performance. Moreover, good thermal conductivity of SiC also allows SiC devices to operate with high current ratings [16]. However, due to relatively complicated production process for SiC power devices, only SiC FET and SiC diodes have become common commercial devices. Regarding SiC-based MBSs, actually, the production process can also be divided into four stages: Substrate preparation, epitaxial layer growth, wafer manufacturing, and packaging, which is similar to that of Si-based MBSs. However, the production process of SiC-based MBSs is more complex, such as the density of microtubule defects in silicon carbide wafers, low efficiency of epitaxial process, special requirements for doping process, and temperature resistance of supporting materials [17]. The difficulty level of expanding SiC crystal growth is also high. As the crystal size increases, the difficulty level of growth process increases geometrically. Therefore, the reasonable and effective sharing of partial structures is an important research content of SiC-based MBSs. Due to the channel formation on the crystal surface of SiC FET structure, which leads to low channel mobility, it is difficult to further reduce the conduction resistance of devices based on this structure.

Compared with SiC and Si devices, the material characteristics of GaN power switches give them relative advantages in reducing turn-ON resistance and turn-OFF time [16]. GaN-MBSs based on HEMT structure are the most widely studied MBSs in published articles. Due to the relatively immature issue of substrate single crystals and the lack of commercially available high-quality independent GaN substrates, the heteroepitaxial defect density of GaN MBSs becomes a key consideration. Compared with other substrates, GaN-based thin films grown on Si substrates are currently the most commonly used method for producing GaN MBSs [14]. Due to the difficulty in obtaining good metal semiconductor Ohmic contact through high doping of GaN materials, the external connection points of GaN MBSs are one of the key issues that need to be studied [18]. Considering that it is difficult to obtain high-quality and large-sized GaN seed crystals, reducing chip volume through shared structures becomes an important research topic for GaN MBSs.

III. Power Integration for MBSs

Traditional BiSs require the combination of several discrete components and semiconductor switches. Although this combination method is inexpensive and easy to implement, the resulting long current-flow path increases the overall impedance and parasitic parameters. Moreover, the series of two or more power devices will also increase the total ON-resistance. These drawbacks will lead to the deterioration of the stability and efficiency of the whole electrical system. Therefore, overcoming the shortcomings of discrete devices is an inevitable problem in the application of BiSs. Although the traditional design through printed circuit boards is still a feasible solution, due to the obvious limitations of this approach, more advanced monolithic integration solutions need to be sought [13]. There are currently two main monolithic integration solutions for bidirectional switches. The first method is to integrate multiple power semiconductors into a module one by one through electrical connections, called UDDC. The second method is to integrate semiconductor components such as switches or diodes into a single chip by sharing and combining partial structures, known as VCD-MI and CCD-MI [8][19].

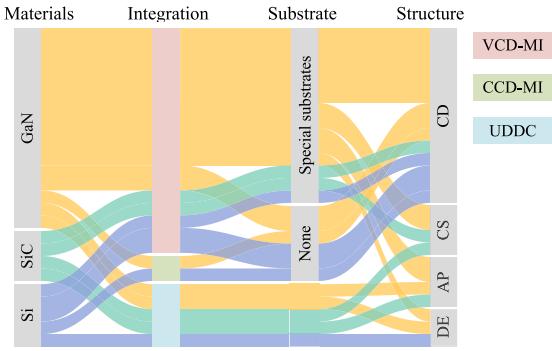

Fig. 3. Literature distribution statistics on materials, power integration schemes, substrates, and circuit structures of MBSs in previous studies.

For UDDC, the layout and heat dissipation of semiconductor power devices are important issues that this monolithic integration method needs to face [20]. Many explorations have been made in various integration methods based on shared part emitters for monolithic bidirectional switches, especially VCD-MI. Due to the fact that two transistors share a portion of the active area, using the dual gate configuration switch can effectively reduce the total chip area. However, dual gate configuration requires two reference points and two gate drive signals to control the MBSs. To simplify the gate driver of MBSs, diode-embedded (DE) configuration of MBSs [21] and common-source (CS) configuration-based single reference bidirectional switches [22] can use only one gate driver. However, these two structures also have significant drawbacks: one is the increase of the voltage drop and ON-state resistance caused by the increase of diodes, and the other drawback is the need to introduce a voltage reference point inside the MBSs. Besides, due to the significant impact of the applied substrate potential and substrate termination method on the transient switching characteristics of WBG switches, it is necessary to select a suitable substrate for the integration implementation.

The Sankey diagram shown in Fig. 3 shows the proportion of structures used for bidirectional switches of different materials. CCD-MI based on thyristor structure was studied in the early

stages, although this power integration technique for MBSs is not the mainstream. Currently, the most popular power integration technique for MBSs is the VCD-MI technique, and the vast majority of them use tailored substrates made of non-GaN materials.

IV. Characteristic Analysis for MBSs

In addition to semiconductor materials and power integration methods, the transistor process implementation and design parameters of MBSs directly affect the electrical performance of MBSs. Therefore, this section mainly analyzes the main electrical characteristics and determining factors of MBSs.

A. Process Implementation of MBSs

The current mainstream transistors include three types: FET, bipolar junction transistor (BJT), and insulated gate bipolar transistor (IGBT). All of them can be used to construct MBSs. Although BJT-based MBSs have the advantage of low noise, they have poor high-voltage resistance and are difficult to adapt to high power application requirements, so they are rarely used in practice.

FET-based MBSs have simple working principle and fast switching speed, which are suitable for application in high-frequency switching conditions. According to the characteristics of GaN devices with FET, strain will be generated at the interface between GaN and AlGaN materials, which can induce two-dimensional electric gas (2DEG) at the interface and effectively conduct electricity. This type of FET with heterojunction is called HEMT. There is no difference in properties between silicon-based FET and GaN based HEMT, and the electrical parameters are only related to the material properties. There are four process implementation methods that enable GaN-based HEMTs. A method that depletes the 2DEG below the gate by injecting fluorine atoms into the AlGaN barrier layer is called gate injection transient (GIT) method. Due to the difficulty in controlling the location and amount of atoms implantation, this method is relatively complex to operate in practice and therefore not the focus of current research. The second method is to deplete the 2DEG under the gate by growing positively charged p-GaN at the top of the AlGaN barrier. This method is relatively easy to implement, making it very suitable for enhanced-mode MBSs that are activated by positive gate voltage. The third method is to thin the AlGaN barrier layer through etching, ultimately eliminating the 2DEG under the gate. This method has lower gate leakage current and process complexity, making it suitable for depletion-mode MBSs. The precise control of etching depth is the most difficult part to break through in this method, which affects the realization of large-scale production. The last method is to combine an enhanced FET and a depletion HEMT, which is usually called cascode. This method can withstand high voltages and is easy to implement, but it has high conduction losses. Therefore, it does not represent the future trend for the development of MBSs.

IGBT-based MBSs essentially adopt hybrid structure, based on a combination of FET and bipolar transistors. They exhibit good high-voltage blocking capability, but its switching frequency and conduction impedance are not as good as FET-based MBSs. Due to the complex PN junction growth required in device process implementation, GaN-IGBT based MBSs cannot easily achieve conductivity control without 2DEG, which limits wider application.

B. Impact of Process Implementation Parameters on MBSs

In addition to the process flow, the process implementation parameters of MBSs will also affect the electrical performance of MBSs to different degrees. Similar as traditional power devices, process parameters such as channel length, channel width, Drain-Source spacing, and doping concentration will inevitably have similar effects on the electrical parameters of MBSs. For example, the shorter channel length of MBSs also makes the switching speed faster, but it may also lead to higher leakage current and more severe short-channel effects. Considering that these impacts are quite common, we will not focus on them here.

MBSs have some unique process parameters. Among them, the spacing between two gates of MBSs is a unique parameter that needs to be considered in the design, which will affect the breakdown voltage and saturation current of MBSs [23]. For MBSs based on vertical device structures such as IGBT-based MBSs, their gates are usually set at the center of both ends of the device. The gate separation is fixed, which cannot be regarded as a design parameter. For MBSs based on horizontal device structures such as HEMT-based MBSs, it is necessary to analyze the influence of gate separation distance. It is the fact that the highest potential point of HEMT-based MBSs is located below the gate, in the direction near the high voltage side. Therefore, changing the gate spacing will inevitably change the distance between the maximum potential points. Specifically, for Schottky contact in MBSs, the positive voltage terminal is located at the far end electrode, and the further the gate is from the low voltage terminal, the higher the breakdown voltage. Thus, the smaller the gate separation spacing, the higher the breakdown voltage. On the contrary, for Ohmic contact in MBSs, the positive voltage terminal is located at the proximal electrode, and the closer the gate is to the low voltage terminal, the lower the breakdown voltage. Thus, the smaller the gate separation spacing, the lower the breakdown voltage. The gate voltage can activate the carrier, so the closer the gate is to the center, i.e., the smaller the gate separation, the better performance of the channel formed, and the electrons are easier to flow through the channel to the electrode. At this point, the saturation current of MBSs is larger. Therefore, the gate separation spacing should be optimized according to the process implementation of MBSs and their main electrical specifications such as the breakdown voltage and saturation current.

V. Physical Structure for MBSs

At present, there are mainly four circuit structures for MBSs: diode-embedded (DE) configuration, antiparallel (AP) configuration, common-drain (CD) configuration, and CS configuration, as shown in Fig. 4. First, as shown in Fig. 4(a), the equivalent circuit of DE structure consists of four diodes and an active

TABLE I
SUMMARY OF MAIN CHARACTERISTICS FOR MBSS BASED ON CD CONFIGURATION

Reference	*Material*	*Structure*	*MBSs type*	V_{max} (V)	$Delay_{on}$ (μs)	*Onstate Voltage*(V)	V_{GS} (V)	R_{on} (Ω/mm^2)	*Switching frequency*(kHz)
[25] [26]	Si	IGBT	VCD-MI	1k	1	0.8	10	NG	NG
[7] [27]	Si	IGBT	VCD-MI	90	NG	3	10	NG	NG
[10]	Si	BJT	CCD-MI	500	NG	NG	-	NG	NG
[28]	Si	FET	VCD-MI	40	NG	3	5	0.06	NG
[5]	GaN	HEMT	VCD-MI	600	0.25	1.3	3	NG	NG
[29]	GaN	HEMT	VCD-MI	650	20	1.5	5	0.31	2
[30] [31]	GaN	HEMT	CCD-MI	600	0.45	NG	5	16.7	1k
[32]	GaN	FET	VCD-MI	500	0.009	3.55	10	NG	1k
[33]	GaN	HEMT	VCD-MI	1340	NG	1	4	42	10
[34]	GaN	FET	VCD-MI	600	0.1	1.5	NG	NG	NG
[35]	GaN	FET	VCD-MI	1000	NG	NG	5	16.7	NG
[19] [36]	GaN	HEMT	VCD-MI	500	0.01	NG	6	450m*	50
[37]	GaN	HEMT	VCD-MI	650	0.8	NG	5	20	NG
[38] [39] [40]	SiC	FET	VCD-MI	1200	0.1	3	20	$4e^{-4}$	50
[41]	SiC	IGBT	VCD-MI	3000	0.5	2	30	14	NG

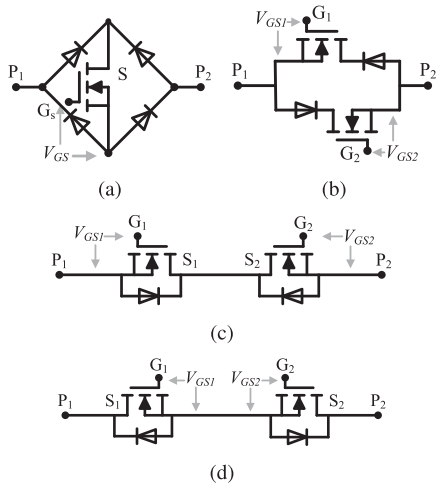

Fig. 4. Four circuit structures for MBSs. (a) Diode-embedded configuration. (b) Antiparallel configuration. (c) Common-drain configuration. (d) Common-source configuration.

switch. By controlling the ON/OFF of the active switch, the power flow of MBSs can be effectively controlled. Moreover, when MBSs are turned ON, the current flows through two diodes and an active switch, resulting in higher turn-ON losses compared to other structures. However, due to the fact that this structure only has one active switch, it is relatively easy to fabricate MBSs and can be easily controlled in practical use. The AP structure is shown in Fig. 4(b). Its equivalent circuit consists of two switches in reverse parallel. Due to the fact that this parallel structure does not require a built-in diode, it can more easily reduce the chip size. However, the low reverse-blocking voltage may become a problem that this topology faces. As shown in Fig. 4(c) and (d), CD and CS configurations are similar and completely symmetrical. The equivalent circuit of the CD and CS structures includes two active switches connected in reverse series and sharing the drain or source. However, the average turn-ON loss of the CD configuration and the average turn-OFF loss of the CS configuration may become slightly higher compared with other structures [24]. For the comparison of CD and CS configurations, CS-based MBSs require an additional reference voltage to achieve the normal switching operation, which will add the design complexity. Therefore, CD configuration has become more popular for the design and optimization of MBSs.

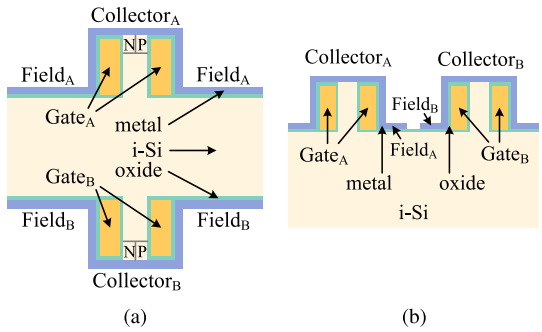

Fig. 5. Schematic illustration of CD-based inchoate MBSs. (a) Longitudinal structure. (b) Lateral structure.

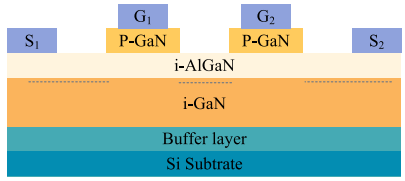

Fig. 6. Schematic illustration of CD-based MBSs with double-gate structure.

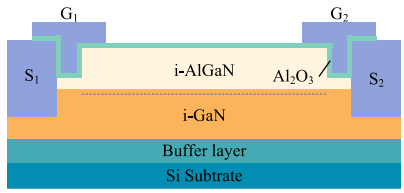

Fig. 7. Schematic illustration of CD-based MBSs with two 2DEG tunnel junctions structure.

A. CD-based MBSs

Table I summarizes the main characteristics for MBSs based on the CD configuration. Typically, there are three categories of schemes for CD-based MBSs, as illustrated in Figs. 5(a), 6, and 7, respectively. Fig. 5(a) shows the first category of schemes for CD-based MBSs. Specifically, a longitudinal silicon based MBS structure was firstly proposed in 2000 [42] and [43]. The upper and lower parts of the switch are completely symmetrical, and the central region is composed of a piece of Si without doped

atoms and recombination centers. To ensure a lower surface generation or recombination speed, each material surface is covered with a high-quality oxide layer. The field electrodes $Field_A$ and $Field_B$ are carried on this layer of oxide. In the top region, there are highly doped n^+ and p^+ regions directly connected to the contact electrodes $Collector_A$ and $Collector_B$, respectively. Finally, gate electrodes $Gate_A$ and $Gate_B$ are connected on the sidewalls of the two protruding areas above and below. This MBS has a simple structure and is easy to achieve bidirectional conduction. Besides, it uses a MOS field-induced accumulation layer as the emitter, thus, it is capable of operating normally in higher temperature ranges and achieving transient control of switches. Subsequently, a prototype of this bidirectional switch was presented in [25] and [26]. However, due to its longitudinal double-sided structure, this switch requires contact points to be set in two spatial dimensions. Based on this, [7] and [27] changed this longitudinal structure to the lateral structure, as shown in the Fig. 5(b). The vast majority of subsequent MBSs also use this structure and its variants. In [28], a new structure of MBSs was presented, which also uses Si as the substrate with the aim to achieve extremely low ON-state resistance.

Fig. 6 illustrates the second category of schemes for CD-based MBSs, which was originated from the above mentioned lateral structure and GIT structure [5]. The dashed line in the figure represents 2DEG and will be represented in the same way in subsequent figures. This structure can achieve bidirectional reverse blocking without the need for additional diodes, which can significantly reduce the ON-state voltage. The top two sides of the structure are two Ohmic electrode terminals S_1 and S_2, with two gate terminals G_1 and G_2 in the middle. There is a p-GaN layer sandwiched between the i-AlGaN layer and two gate terminals to ensure the normal shutdown of the switch. The external input signal of G_1 can control the opening and closing of electron flow from S_1 to S_2, while the external input signal of G_2 can control the opening and closing of electron flow from S_2 to S_1. [29] and [33]–[37] also adopts a similar structure. To be specific, [33] exhibits a higher breakdown voltage, and [35] has a lower switching delay with fairly small chip size, 94 mm^2. It should be noted that the overall ON-state resistance of MBSs proposed by [36] is 450 mΩ. The authors in [30] and [31] also used the GIT structure to form MBSs. The switch integrates an isolated gate driver circuit internally, allowing it to achieve the switching function at a very small chip size, but increasing the chip area to 306 mm^2.

Fig. 7 illustrates the third category of schemes for CD-based MBSs, where a normally closed MBSs with two 2DEG tunnel junctions at two interfaces S_1 and S_2, respectively [32]. Compared to MBSs containing Ohmic contacts that must be manufactured at high temperatures, this category of MBSs does not exhibit an obvious degeneration in ON-state losses. Moreover, this structure exhibits extremely low switching delay and can operate normally at extremely high switching frequencies.

Table II summarizes key research directions for MBSs based on the CD configuration. It is noticed that only one SiC-based MBS with the CD configuration was reported, which exhibits extremely high withstanding voltage and extremely low ON-state resistance.

TABLE II
KEY RESEARCH DIRECTIONS FOR CD-BASED MBSS

	IGBT	FET	HEMT
Switching frequency	[32]	-	[30] [31]
Breakdown voltage	[25] [26] [33]	[35] [38]- [40]	-
On state resistance	-	[34] [38]- [40]	[29]
Other	[7] [27]	[37]	[5]

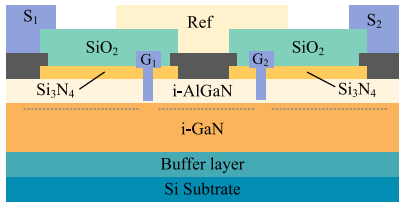

Fig. 8. Schematic illustration of CS-based MBSs.

B. CS-based MBSs

Table III summarizes main characteristics for MBSs based on the CD configuration. Fig. 8 illustrates the typical structure for CS-based MBSs [22], [44], and [45]. Because the driving signal of CS-based MBSs is generally controlled by the voltage difference between the source and the gate, which is different from the CD-based MBSs, CS-based MBSs need to introduce an additional port in the device to provide the source level voltage reference required by the drive circuit. Compared to the structure shown in Fig. 7, this structure is similar but adds an external contact point "Ref" at the center of the chip to provide source voltage for the driving circuit. In addition, this structure uses Si_3N_4 to replace the commonly used p-type doped GaN. In the literature, this structure is used to achieve two MBSs with the maximum operating voltage of 250 V and 150 V, respectively, and their total conduction resistances are 700 mΩ and 1100 mΩ, respectively. In [46], another GaN-based MBSs that uses a similar structure was proposed, although it has a lower operating voltage, it can operate normally at extremely high switching frequencies.

Regarding SiC-MBSs based on the CS configuration, a scheme through the physical connection of existing SiC-based FETs and encapsulated in the chip was proposed [48]. The chip introduces two FETs that share one source for the external use. Considering the application of circuit breakers, the main design focus of achieving high blocking voltage [47], [48]. Specifically, the chip area should be increased to withstand a high voltage and meet the heat dissipation requirement. At the same time, this component also exhibits low ON-state resistance.

C. AP-based MBSs

The blue section in Table IV summarizes the main features of MBSs based on the AP configuration. AP-based MBSs usually consist of two switching structures connected in reverse parallel, which can achieve unidirectional conduction and reverse blocking. The transverse section diagram of the AP-based MBSs and the key longitudinal section diagram of one of the switching structures are shown in Fig. 9. And the gate signal needs to use

TABLE III
SUMMARY OF MAIN CHARACTERISTICS FOR MBSS BASED ON CS CONFIGURATION

Reference	*Material*	*Structure*	*MBSs type*	V_{max} (V)	$Delay_{on}$ (μs)	*Onstate Voltage*(V)	V_{GS} (V)	R_{on} (Ω/mm^2)	*Switching frequency*(kHz)
[22] [44] [45]	GaN	HEMT	VCD-MI	250/450	0.02	NG	6	700/1100m*	1k
[46]	GaN	HEMT	VCD-MI	NG	0.023	4	6	NG	40k
[47]	SiC	FET	VCD-MI	1.2k	NG	NG	2.5	NG	1
[48]	SiC	FET	UDDC	1.2k	NG	NG	NG	$7e^{-3}$	NG

TABLE IV
SUMMARY OF MAIN CHARACTERISTICS FOR MBSS BASED ON AP OR DE CONFIGURATION

Reference	*Configuration*	*Material*	*Structure*	*MBSs type*	V_{max} (V)	$Delay_{on}$ (μs)	*Onstate Voltage*(V)	V_{GS} (V)	R_{on} (Ω/mm^2)	*Switching frequency*(kHz)
[49]	AP	GaN	HEMT	VCD-MI	650	4.8	0.63	7	30	2
[50]	AP	GaN	HEMT	VCD-MI	790	NG	0.6	5	18	NG
[51]	AP	GaN	FET	UDDC	NG	NG	NG	5.6	NG	25k
[52]	AP	SiGe	DPDT	UDDC	NG	NG	NG	2.5	25	22k
[21]	DE	GaN	FET	VCD-MI	945	12	1	12	385	1
[53]	DE	GaN	FET	UDDC	790	3	0.6	5	NG	0.5
[20]	DE	Si	IGBT	UDDC	4.5k	NG	2.4	20	NG	NG

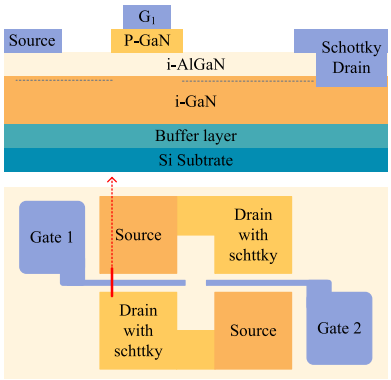

Fig. 9. Schematic illustration of AP-based MBSs.

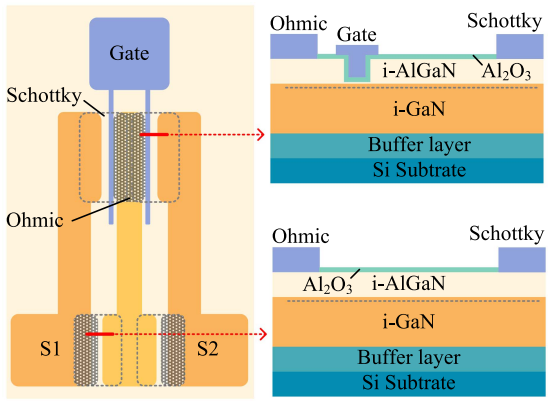

Fig. 10. Schematic illustration of MBSs with DE configuration.

the voltage at both ends of the MBSs as a reference to achieve its control [49]. An i-GaN layer and an i-AlGaN layer are arranged above the substrate and buffer layer of silicon. A p-GaN layer is sandwiched between the i-AlGaN layer and the gate to ensure normal shutdown of the switch. The source is directly connected to the i-AlGaN layer, and the drain with Schottky is connected to the i-GaN layer. The advantage of this structure lies in its lower ON-state voltage. Lei et al. [50] uses a longitudinal section similar to Fig. 7, which shows better electrical performance compared to [49].

Based on UDDC, [51] and [52] integrate components such as capacitors, inductors, and power switches into the chip. They have a similar research focus, which is to achieve extremely high switching frequencies on smaller chips. Considering structural limitations, this design is unable to withstand high voltage, which limits their application scopes.

D. DE-based MBSs

DE-based MBSs have natural disadvantages, such as high ON state resistance, complex electrical structure, and uncontrolled power flow direction. Although they have advantages such as fast switching speed and easy control, they have been only studied in limited fields. The yellow section in Table IV summarizes the main features of MBSs based on the DE configuration.

Based on the DE configuration, [21] has proposed a MBSs with a transverse section as shown in Fig. 10. Four Schottky and three Ohmic are embedded in the chip. On the silicon substrate, there are i-GaN layers and i-AlGaN layers, followed by the p-GaN layer and oxide layer at the top. The two Ohmic connected to S_1 and S_2, as well as the two Schottky bases in the middle, are respectively connected to the p-GaN layer. The longitudinal cross-sectional structure of the part connected to the gate on the other side is similar to Fig. 7. Gate and Al_2O_3 pass through the p-GaN layer and come into contact with the i-AlGaN layer. This type of component can operate normally at relatively high voltage levels, but its construction also leads to a high ON-state resistance.

In UDDC DE-based MBSs, the comprehensive performance of MBSs proposed in [20] is better than that of [53]. The MBSs proposed in [20], which are applied to solid-state circuit breakers (SSCBs), connect commercial IGBTs with resistors, capacitors, and diodes to achieve ultrahigh voltage withstand at a lower cost.

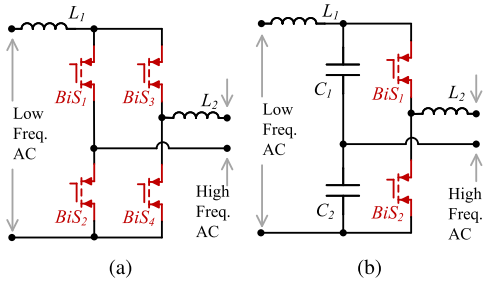

Fig. 11. Applications of MBSs in Dual Active Bridge Converters. (a) Full-bridge Version. (b) Half-bridge Version.

VI. Typical Applications for MBSs

In this section, typical applications of monolithic bidirectional switches (MBSs) will be systematically summarized in order to fully explore the advantages of MBSs, including small internal parasitic parameters, reduced conduction resistance, and fast switching frequency.

A. Dual Active Bridge Converter

Fig. 11 illustrates main applications of MBSs in dual active bridge (DAB) converters, including both full-bridge-based DAB converters and half-bridge-based DAB converters. Main application of MBSs-based DAB converters covers both dc–dc and dc–ac power conversions. In [54], an asymmetric DAB converter with MBSs was introduced. As shown in Fig. 11(a), it has a set of MBSs on the primary side of the transformer, and utilizes the phase shift control with a constant switching frequency. This MBSs-based DAB converter has the capability of reducing the high cycle energy and high conduction loss, which are regarded as key issues of existing symmetric topologies through the phase shift control. Thus, it is suitable for the applications with the requirement of high gain or current isolation. [55] also adopts this MBSs-based DAB converters and compares two types of control strategies, including the shot through duty cycle control and reverse energy transfer duty cycle control. Different control strategies are provided for achieving soft switching while requiring higher efficiency or smaller input ripple or higher voltage gain. In [56], an ac–dc converter was proposed based on Fig. 11(b), which can not only control the dc output voltage or current, but also control the ac grid current through a single conversion stage, helping to achieve higher power density with lower complexity. The primary side voltage of a transformer is a square wave voltage with an amplitude of $|v_i|/2$ that varies over time. The secondary voltage V_s of the transformer is composed of positive and negative voltage pulses with an amplitude of V_o. Ref. [57] reshapes the transformer leakage current i_{L_σ} through changing the control logic to achieve zero voltage switching. For MBSs used on bridge circuit topologies, they typically require high-frequency operation at high operating voltages, so HEMT-MBSs based CS and CD configurations have more advantages.

MBSs can also be utilized for the efficiency improvement of DAB converters. It is well known that power semiconductor devices typically exhibit switching losses due to hard switching especially with the increase of the switching frequencies for WBG devices. These losses can be reduced by adjusting control strategies or adding auxiliary absorption circuits. In [58], a MBS connected in series on the transformer winding constitutes the current feed circuit shown in Fig. 12, and the energy return is controlled by isolating the leakage inductance of the transformer and the MBS, so as to realize the zero voltage switching of the transistor at the voltage feeding side. Applying MBSs to such a structure can greatly reduce the energy cycling, allowing only the energy stored in the leakage inductance to return to the power supply side.

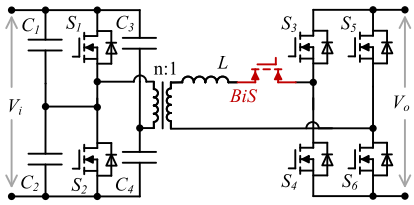

Fig. 12. Efficiency improvement for DAB converters with MBSs connected in series with the transformer winding.

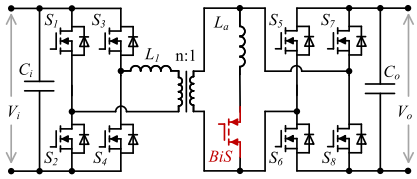

Fig. 13. Efficiency improvement for DAB converters with MBSs in parallel with the transformer winding.

The dc bias current and cyclic current limit conventional DAB converters in asymmetric PWM control, causing greater conduction losses. In order to achieve a tunable resonant circuit for DAB converters, [59] introduced an improved *LCL* resonant circuit with switch controlled inductance, as shown in Fig. 13. This MBSs-based structure can generate a symmetrical resonant current of zero dc offset current independent of duty cycle changes, thereby reducing the conduction loss of the entire system and extending its service life at the cost of slightly increasing the prototype volume and control complexity.

MBSs used in these two situations are usually used in low voltage, and low on resistance is particularly important for this application scenario. Therefore, MBSs based on AP configuration have a simple structure and low conduction impedance, making them more suitable for use in this situation.

B. Solid-State Circuit Breaker

Compared to mechanical circuit breakers, SSCBs have advantages such as no arcing, short response time, long service life, high reliability, and low maintenance costs. In energy storage systems, due to the bidirectional flow of energy, bidirectional circuit breakers are highly demanded to adapt to the system, and the design based on bidirectional switches is one of the important branches of bidirectional circuit breaker design [60]. As shown

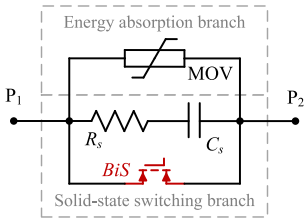

Fig. 14. Applications of MBSs in Solid-state Circuit Breakers.

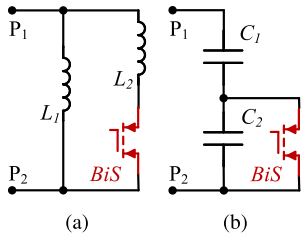

Fig. 15. Applications of MBSs in variable inductance and capacitance topology. (a) Variable Inductance. (b) Variable Capacitance.

in Fig. 14, a circuit breaker based on a bidirectional switch includes a solid-state switching branch and an energy absorption branch. When the system is operating normally, the bidirectional switch is in a conductive state. When a short circuit fault occurs in the system, the bidirectional switch turns OFF, and the fault energy is absorbed by the energy absorption branch [61]. There are generally two key design focuses for MBSs-based SSCBs: One of them is the ON-state resistance and power loss minimization, the other is the switching frequency increase to prevent the short-circuit fault current and surge voltage [62]. Researches in [37], [47], [48] show that MBSs-based on WBG materials can construct SSCBs with high power density due to compact device structure, fast switching, and low ON-state resistance for MBSs. MBSs used in SSCBs always maintain their ON-state when the system is not faulty, and need to be able to withstand large surge voltages in the event of system faults. Furthermore, they usually do not have harsh volume requirements. Therefore, under the premise of small ON-state impedance, the IGBT-based UDDC structure MBSs with the best voltage resistance is the most suitable.

C. Variable Capacitance or Inductance

Achieving the soft-switching operation for a complete range of power and voltage is essential for power converters. However, due to fixed capacitance or inductance in power converters, this task becomes challenging. For instance, in [63], when the duty cycle is below 0.5, the energy stored in L_1 is insufficient to discharge the current to zero in boost mode, or charge the voltage to V_{P1} in boost mode, which will result in the inability to achieve soft switching operation. At this point, auxiliary components, as shown in Fig. 15(a), can be added to provide soft switching conditions for the auxiliary switch at both the OFF and ON times. For instance, in [64], a variable inductor that is composed of a resonant inductor and a MBS was adopted in a traditional bidirectional converter. The research shows that a wide range of soft-switching operation can be achieved by exciting L_2 in the auxiliary circuit with a voltage difference "$V_{P1}-V_{P2}$" before turning ON the main switch.

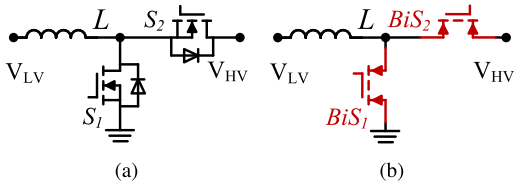

Fig. 16. Applications of MBSs in bidirectional choppers. (a) Bidirectional DC choppers. (b) Bidirectional AC choppers.

Similarly, variable capacitors are highly required for power factor correction and soft switching range expansion. Traditional compensation networks with fixed compensation capacitance values are incapable of maintaining high power factor and system efficiency simultaneously when deviating from pre-set coupling conditions. In some cases, the power factor can be guaranteed, but the soft switching capability on the main bridge cannot be maintained due to changes in output voltage caused by different load power angles [65]. At this point, adding a variable capacitor consisting of a fixed capacitor and a MBS, as shown in Fig. 15(c), can change the effective resonant capacitance by controlling the conduction angle of the switch. Specifically, the overall capacitance of the structure shown in Fig. 15(c) is adjustable to compensate for the increase in inductance caused by poor coupling conditions. For instance, in the case of poor coupling, with the increase of the magnetization and leakage inductance, the conduction angle of the MBS can be reduced to obtain high capacitance. In the case of good coupling, the conduction angle of the MBS will be increased to obtain low capacitance [66]. At this point, when the load environment changes, the power factor of the system can be always maintained at a high level within a certain range. Besides, a wide range of soft-switching operation and minimum circulating current under a wide range of the output voltage and current can be achieved due to the introduction of MBSs. This structure, which requires very low performance of bidirectional switches, is often found in circuits as part of a small application. Therefore, MBSs based on the CS and CD configurations whose chip size is smaller and the DE configuration who is easy to control are suitable for these applications.

D. Bidirectional AC Chopper

A bidirectional dc power conversion unit, also known as a dc chopper, usually consists of an inductor and two switches, as shown in Fig. 16(a). It can operate in both the boost mode with the energy ac from LV to HV and the buck mode with the energy flowing from HV to LV. Thus, a bidirectional ac power conversion unit, also know as the ac chopper, needs to switch between boost and buck modes at least four times during the power source cycle, which complicated the control and increase the power loss [67].

With the MBSs, the ac chopper and its variants in Fig. 16(b) can be used in direct ac motor drive or un-interruptible power supply systems. Due to the fact that this topology can completely

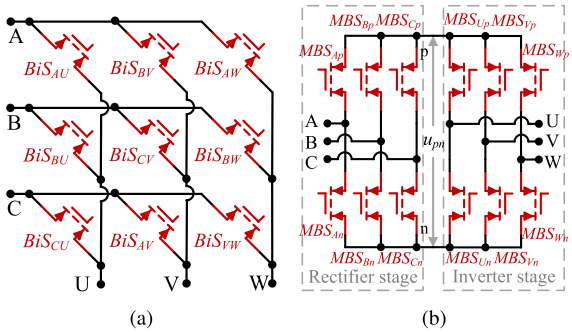

Fig. 17. Applications of MBSs in AC matrix converters. (a) Direct matrix converters. (b) Indirect matrix converters.

block the power transmission by turning OFF MBS_2, it can be used as a protection circuit to prevent fault propagation in the event of a fault on one side. The replacement of MBSs enables the topology to operate in four quadrants with small volume. Furthermore, the phase angle between voltage and current can exceed 90° to achieve flexible bidirectional power transmission [68]. This simple structure also requires less performance parameters from MBSs. Therefore, CS and CD configurations MBSs who is more suitable for miniaturized is better suited to this application.

E. Matrix Converter

One of the most important applications of MBSs is the matrix converter, which is considered the most effective ac–ac conversion topology due to single-stage power conversion. It exhibits an obvious advantage of reducing various operational losses compared with traditional two-stage ac–dc–ac conversion. Actually, there are two configurations for the ac–ac matrix converters: One is the indirect matrix converter (IMC), as shown in Fig. 17(a) [69]. It has a back-to-back configuration of a current source rectifier and a voltage source inverter, without energy storage capacitors in the voltage dc link, which is beneficial for improving system life and power density. The other configuration of the ac–ac matrix converter is the direct matrix converter (DMC), as shown in Fig. 17(b). It can be regarded as an integrated version of IMC, which requires fewer semiconductor devices since the device number can be reduced from 12 to 9. The most critical component among the different configurations of matrix converters is the bidirectional switch, which alternates between the ON and OFF states at a relatively high switching frequency within a cycle to achieve direct ac–ac power conversion [70]. More three-phase ac converters applying MBSs are described in detail in [71] and [72], which will not be discussed in this article. And there are the same performance requirements for the applied MBSs. Compared with UDDC-based bidirectional switches, MBSs based on WBG semiconductor materials exhibit more advantages for the application in matrix converters since they can will significantly reduce the ON-state resistance, minimize the parasitic inductance, improve the power density and reliability. However, MBSs based on CCD-MI and VCD-MI still need to improve the ability of reverse voltage resistance. With the availability of MBSs, the matrix converter especially DMC has become a highly attractive scheme for ac–ac power conversion and variable-speed drives due to the minimal device count.

VII. Conclusion

MBSs have excellent performance and broad application prospects. Especially with the popularity of WBG semiconductor materials, MBSs based on SiC or GaN exhibit high-frequency switching while reducing parasitic inductance and conduction resistance. This article analyses main characteristics and challenges brought by MBSs and their power integrated techniques especially for the emerging WBG devices. Besides, this article provides a comprehensive comparison of various MBSs from the perspectives of materials, physical structures, characteristics, and applications.

In this article, three main power integration schemes for BiSs, including UDDC, VCD-MI, and CCD-MI, have been systematically reviewed. The research shows that main design issues of UDDC-based BiSs are the reduction of parasitic inductance and heat dissipation, while the corresponding design challenges for VCD-MI based BiSs and CCD-MI based BiSs are substrate epitaxy, gate structure, process parameter selection, and process consistency control.

In addition to three commonly-used semiconductor materials for MBSs, the article also systematically discusses four physical structures for MBSs: DE configuration, AP configuration, CD configuration, and CS configuration. Among four structures, the CD configuration is the most popular structure. The CD configuration is more valuable than the CS configuration because it does not require additional voltage reference points The AP configuration can also achieve normal operation at high frequencies, but its structure makes it difficult to achieve high reverse blocking voltage. The DE configuration can achieve bidirectional conduction in a simple control method, but it cannot control the direction of the power flow. Besides, it has a large opening resistance. This characteristic makes it very suitable for circuits that require quick opening or closing, such as circuit breakers. Finally, this article provides an overview of main applications for MBSs, including matrix converters, dual-active-bridge converters, variable inductor or capacitor, bidirectional ac chopper, and solid-state circuit breakers.

To the knowledge of authors, this article is the first article for a comprehensive review of WBG-based MBSs compared with prior review and survey articles on characteristics and applications of WBG devices. The review of this article will provide good design reference and guidance for the latest MBSs especially especially for the emerging WBG devices. Besides, this review article is expected to facilitate the MBS structure design and in-depth optimization, which is essential for the future large-scale promotion of MBSs.

References

[1] Y. Xu, Z. Wang, P. Liu, Q. Wei, F. Deng, and Z. Zou, "The modular current-fed high-frequency isolated matrix converters for wind energy conversion," *IEEE Trans. Power Electron.*, vol. 37, no. 4, pp. 4779–4791, Apr. 2022.

[2] L. Xing, Q. Wei, and Y. Li, "Transformerless series-connected current source converter," *IEEE Trans. Power Electron.*, vol. 37, no. 8, pp. 8811–8815, Aug. 2022.

[3] H.-S. Kim, Y.-C. Kwon, S.-J. Chee, and S.-K. Sul, "Analysis and compensation of inverter nonlinearity for three-level T-type inverters," *IEEE Trans. Power Electron.*, vol. 32, no. 6, pp. 4970–4980, Jun. 2017.

[4] C. Benboujema, A. Schellmanns, N. Batut, J. B. Quoirin, and L. Ventura, "Low losses bidirectional switch for ac mains," in *Proc. 2009 13th Eur. Conf. Power Electron. Appl.*, 2009, pp. 1–10.

[5] T. Ide, M. Shimizu, X.-Q. Shen, T. Morita, T. Ueda, and T. Tanaka, "Equivalent circuit model for a GaN gate injection transistor bidirectional switch," *IEEE Trans. Electron Devices*, vol. 59, no. 10, pp. 2643–2649, Oct. 2012.

[6] A. Bourennane, M. Breil, J.-L. Sanchez, P. Austin, and J. Jalade, "A new triggering mode in a vertical bi-directional MOS-thyristor device," *Microelectronics J.*, vol. 35, no. 3, pp. 277–285, 2004.

[7] M. Baus et al., "Fabrication of monolithic bidirectional switch (MBS) devices with MOS-controlled emitter structures," in *Proc. 2006 IEEE Int. Symp. Power Semicond. Devices IC's*, 2006, pp. 1–4.

[8] A. Bourennane, H. Tahir, J. Sanchez, L. Pont, G. Sarrabayrouse, and E. Imbernon, "High temperature wafer bonding technique for the realization of a voltage and current bidirectional IGBT," in *Proc. IEEE 23rd Int. Symp. Power Semicond. Devices ICs*, 2011, pp. 140–143.

[9] L. V. Phung, F. Ihuel, N. Batut, J.-B. Quoirin, A. Schellmanns, and L. Ventura, "Modelling of a symmetrical bipolar monolithic bidirectional switch," in *Proc. IEEE 2009 13th Eur. Conf. Power Electron. Appl.*., 2009, pp. 1–9.

[10] L. V. Phung et al., "Modeling of a new SOI bidirectional bipolar junction transistor for low-loss household appliances," *IEEE Trans. Electron Devices*, vol. 58, no. 4, pp. 1164–1169, Apr. 2011.

[11] H. Rizk, A. Bourennane, M. Breil, and J.-P. Laur, "Bipolar AC switch for specific mains applications: Design, realization, and characterization," *IEEE Trans. Electron Devices*, vol. 66, no. 9, pp. 3704–3709, Sep. 2019.

[12] B. Zhang and S. Wang, "A survey of EMI research in power electronics systems with wide-bandgap semiconductor devices," *IEEE Trans. Emerg. Sel. Topics Power Electron.*, vol. 8, no. 1, pp. 626–643, Mar. 2020.

[13] C. Kuring, O. Hilt, J. Böcker, M. Wolf, S. Dieckerhoff, and J. Würfl, "Novel monolithically integrated bidirectional GaN HEMT," in *Proc. 2018 IEEE Energy Convers. Congr. Expo.*, 2018, pp. 876–883.

[14] G. E. Mejia-Ruiz, M. R. A. Paternina, A. Zamora-Mendez, J. C. Rosas-Caro, and G. Bolivar-Ortiz, "A novel GaN-based solid-state circuit breaker with voltage overshoot suppression," *IEEE Trans. Ind. Electron.*, vol. 69, no. 9, pp. 8949–8960, Sep. 2022.

[15] Y. Sato, Y. Tanaka, A. Fukui, M. Yamasaki, and H. Ohashi, "SiC-SIT circuit breakers with controllable interruption voltage for 400-V dc distribution systems," *IEEE Trans. Power Electron.*, vol. 29, no. 5, pp. 2597–2605, May 2014.

[16] J. Millán, P. Godignon, X. Perpiñà, A. Pérez-Tomás, and J. Rebollo, "A survey of wide bandgap power semiconductor devices," *IEEE Trans. Power Electron.*, vol. 29, no. 5, pp. 2155–2163, May 2014.

[17] M. Ostling, S.-M. Koo, S.-K. Lee, E. Danielsson, and C.-M. Zetterling, "Recent advances and issues in SiC process and device technologies," in *Proc. 2001 6th Int. Conf. Solid-State Integr. Circuit Technol., Proc. (Cat. No.01EX443)*, 2001, vol. 2, pp. 1173–1178.

[18] M.-Y. Fan et al., "Ultra-low contact resistivity of $< 0.1\Omega\cdot$ mm for Au-free Ti_xAl_y alloy contact on non-recessed i-AlGaN/GaN," *IEEE Electron Device Lett.*, vol. 41, no. 1, pp. 143–146, Jan. 2020.

[19] C. Kuring et al., "Impact of substrate termination on dynamic on-state characteristics of a normally-off monolithically integrated bidirectional GaN HEMT," in *Proc. 2019 IEEE Energy Convers. Congr. Expo.*, 2019, pp. 824–831.

[20] T. Wei et al., "Design and test of the bidirectional solid-state switch for an 160kV/9kA hybrid dc circuit breaker," in *Proc. 2018 IEEE Appl. Power Electron. Conf. Expo.*, 2018, pp. 141–148.

[21] B.-R. Park, S.-W. Han, and H.-Y. Cha, "Diode bridge embedded AlGaN/GaN bidirectional switch," *IEEE Electron Device Lett.*, vol. 36, no. 4, pp. 324–326, Apr. 2015.

[22] S. Léo, F. Jean-Paul, F. David, J. Pierre-Olivier, P. Pierre, and L. Othman, "Implementation of monolithic bidirectional switches in a ac/dc dual active bridge in ZVS auto-switching mode," in *Proc. 2018 IEEE Int. Conf. Ind. Technol.*, 2018, pp. 742–746.

[23] F. Li et al., "TCAD simulation of dual-gate p-GaN/AlGaN/GaN HEMT bidirectional switch," in *Proc. 2021 18th China Int. Forum Solid State Lighting 2021 7th Int. Forum Wide Bandgap Semicond. (SSLChina: IFWS)*, 2021, pp. 49–52.

[24] A. Kanale et al., "Comparison of the capacitances and switching losses of 1.2 kV common-source and common- drain bidirectional switch topologies," in *Proc. 2021 IEEE 8th Workshop Wide Bandgap Power Devices Appl.*, 2021, pp. 112–117.

[25] F. Heinke and R. Sittig, "The monolithic bidirectional switch (MBS) in a matrix converter application," in *Proc. Proc. 13th Int. Symp. Power Semicond. Devices ICs IPSD'01 (IEEE Cat. No.01CH37216)*, 2001, pp. 367–371.

[26] F. Heinke and R. Sittig, "The monolithic bidirectional switch (MBS)," in *Proc. 12th Int. Symp. Power Semicond. Devices ICs. Proc. (Cat. No. 00CH37094)*, 2000, pp. 237–240.

[27] O. W. B. S. M. C . L. M. Baus, M. Z. Ali, and H. Kurz, "Monolithic bidirectional switch (MBS) - a novel MOS-based power device," in *Proc. ESSDERC 2005: 35th Eur. solid-state device Res. Conf.*, 2005, pp. 473–476. [Online]. Available: https://www.research-collection.ethz.ch/handle/20.500.11850/591486

[28] P. Boos, A. Mels, and S. Sque, "A 30V bidirectional power switch in a CMOS technology using standard gate oxide," in *Proc. 2016 28th Int. Symp. Power Semicond. Devices ICs*, 2016, pp. 247–250.

[29] T. Morita et al., "650 V 3.1 mωcm^2 GaN-based monolithic bidirectional switch using normally-off gate injection transistor," in *Proc. 2007 IEEE Int. Electron Devices Meeting*, 2007, pp. 865–868.

[30] S. Nagai et al., "A compact GaN bi-directional switching diode with a GaN bi-directional power switch and an isolated gate driver," in *Proc. 2016 28th Int. Symp. Power Semicond. Devices ICs*, 2016, pp. 183–186.

[31] S. Nagai, Y. Kawai, O. Tabata, S. Choe, N. Negoro, and T. Ueda, "A high-efficient driving isolated drive-by-microwave half-bridge gate driver for a GaN inverter," in *Proc. 2016 IEEE Appl. Power Electron. Conf. Expo.*, 2016, pp. 2051–2054.

[32] Y. Shi, W. Chen, Q. Zhou, and B. Zhang, "A non-ohmic normally-off GaN monolithic bidirectional switch with mis field effect schottky tunnel junction," *Superlattices Microstructures*, vol. 109, pp. 414–422, 2017. [Online]. Available: https://www.sciencedirect.com/science/article/pii/S0749603617305980

[33] H. Umeda et al., "High power 3-phase to 3-phase matrix converter using dual-gate GaN bidirectional switches," in *Proc. 2018 IEEE Appl. Power Electron. Conf. Expo.*, 2018, pp. 894–897.

[34] N. Nain, S. Walser, J. Huber, K. K. Leong, and J. W. Kolar, "Self-reverse-blocking control of dual-gate monolithic bidirectional GaN switch with quasi-ohmic on-state characteristic," *IEEE Trans. Power Electron.*, vol. 37, no. 9, pp. 10091–10094, Sep. 2022.

[35] M. Wolf, O. Hilt, and J. Würfl, "Gate control scheme of monolithically integrated normally off bidirectional 600-v GaN HFETs," *IEEE Trans. Electron Devices*, vol. 65, no. 9, pp. 3878–3883, Sep. 2018.

[36] C. Kuring et al., "Active substrate termination of discrete and monolithic bidirectional GaN HEMTs in a t-type inverter," in *Proc. 2022 24th Eur. Conf. Power Electron. Appl. (EPE'22 ECCE Europe)*, 2022, pp. P.1–P.11.

[37] Z. J. Shen et al., "First experimental demonstration of solid state circuit breaker (SSCB) using 650V GaN-based monolithic bidirectional switch," in *Proc. 2016 28th Int. Symp. Power Semicond. Devices ICs*, 2016, pp. 79–82.

[38] A. Kanale et al., "Switching characteristics of a 1.2 kV, 50 mω SiC monolithic bidirectional field effect transistor (BiDFET) with integrated JBS diodes," in *Proc. 2021 IEEE Appl. Power Electron. Conf. Expo.*, 2021, pp. 1267–1274.

[39] S. S. Shah et al., "Optimized ac/dc dual active bridge converter using monolithic SiC bidirectional FET (BiDFET) for solar PV applications," in *Proc. 2021 IEEE Energy Convers. Congr. Expo.*, 2021, pp. 568–575.

[40] K. Han et al., "Monolithic 4-terminal 1.2 kV/20 a 4H-SiC bi-directional field effect transistor (BiDFET) with integrated JBS diodes," in *Proc. 2020 32nd Int. Symp. Power Semicond. Devices ICs*, 2020, pp. 242–245.

[41] S. Chowdhury, C. W. Hitchcock, Z. Stum, R. P. Dahal, I. B. Bhat, and T. P. Chow, "Operating principles, design considerations, and experimental characteristics of high-voltage 4H-SiC bidirectional IGBTs," *IEEE Trans. Electron Devices*, vol. 64, no. 3, pp. 888–896, Mar. 2017.

[42] R. Sittig and F. Heinke, "Monolithic bidirectional switch.: I device concept," *Solid-State Electron.*, vol. 44, no. 8, pp. 1387–1392, 2000. [Online]. Available: https://www.sciencedirect.com/science/article/pii/S0038110100000782

[43] F. Heinke and R. Sittig, "Monolithic bidirectional switch.: Ii simulation of device characteristics," *Solid-State Electron.*, vol. 44, no. 8, pp. 1393–1398, 2000. [Online]. Available: https://www.sciencedirect.com/science/article/pii/S0038110100000794

[44] D. Bergogne, O. Ladhari, L. S. C. Gillot, R. Escoffier, and W. Vandendaele, "The single reference bi-directional GaN HEMT AC switch," in *Proc. 2015 17th Eur. Conf. Power Electron. Appl. (EPE'15 ECCE-Europe)*, 2015, pp. 1–7.

[45] D. Bergogne et al., "Demonstration of the normally-off bi-directional GaN AC switch," in *2016 Int. Conf. Elect. Syst. Aircraft, Railway, Ship Propulsion Road Veh. Int. Transp. Electrific. Conf.*, 2016, pp. 1–4.

[46] G. Tang et al., "Digital integrated circuits on an E-mode GaN power HEMT platform," *IEEE Electron Device Lett.*, vol. 38, no. 9, pp. 1282–1285, Sep. 2017.

[47] V. Veliadis, B. Steiner, K. Lawson, S. B. Bayne, D. Urciuoli, and H. C. Ha, "Suitability of N-ON recessed implanted gate vertical-channel SiC JFETs for optically triggered 1200 v solid-state-circuit-breakers," in *Proc. 2015 IEEE 3rd Workshop Wide Bandgap Power Devices Appl.*, 2015, pp. 162–165.

[48] P. Cova et al., "Thermal design and characterization of a modular integrated liquid cooled 1200v-35a SiC MOSFET bi-directional switch," *Microelectronics Rel.*, vol. 76-77, pp. 277–281, 2017. [Online]. Available: https://www.sciencedirect.com/science/article/pii/S0026271417302500

[49] H. Wang et al., "Experimental demonstration of monolithic bidirectional switch with anti-paralleled reverse blocking P-GaN HEMTs," *IEEE Electron Device Lett.*, vol. 42, no. 9, pp. 1264–1267, Sep. 2021.

[50] J. Lei et al., "Reverse-blocking normally-OFF GaN double-channel MOS-HEMT with low reverse leakage current and low ON-state resistance," *IEEE Electron Device Lett.*, vol. 39, no. 7, pp. 1003–1006, Jul. 2018.

[51] H. Mizutani, R. Ishikawa, and K. Honjo, "A novel GaN/SiC MMIC gain switch using a resonant bidirectional FET amplifier," in *Proc. 2021 51st Eur. Microw. Conf.*, 2022, pp. 285–288.

[52] M.-K. Cho, I. Song, J.-G. Kim, and J. D. Cressler, "An active bi-directional sige dpdt switch with multi-octave bandwidth," *IEEE Microw. Wireless Compon. Lett.*, vol. 26, no. 4, pp. 279–281, Apr. 2016.

[53] G. Venkataramanan and N. Kogalur, "A hybrid 4-quadrant switch for ac power conversion," in *Proc. 2019 IEEE Energy Convers. Congr. Expo.*, 2019, pp. 5487–5493.

[54] A. Blinov, R. Kosenko, A. Chub, and D. Vinnikov, "Bidirectional soft switching current source dc-dc converter for residential dc microgrids," in *Proc. IECON 2018-44th Annu. Conf. IEEE Ind. Electron. Soc.*, 2018, pp. 6059–6064.

[55] R. Kosenko, A. Chub, and A. Blinov, "Comparison and verification of boost control methods for full soft-switching bidirectional current-fed isolated full-bridge dc-dc converter," in *Proc. 2016 2nd Int. Young Scientists Forum Appl. Phys. Eng.*, 2016, pp. 6–9.

[56] N. D. Dao and D.-C. Lee, "Modulation and control of single-stage bidirectional isolated direct-matrix-based AC-DC converters," in *Proc. 10th Int. Conf. Power Electron. ECCE Asia (ICPE 2019 - ECCE Asia)*, 2019, pp. 2278–2283.

[57] F. Jauch and J. Biela, "Single-phase single-stage bidirectional isolated ZVS AC-DC converter with PFC," in *Proc. 15th Int. Power Electron. Motion Control Conf.*, 2012, pp. LS5d.1–1–LS5d.1–8.

[58] V. Ivakhno, V. Zamaruiev, B. Styslo, R. Kosenko, and A. Blinov, "Bidirectional isolated ZVS DC-DC converter with auxiliary active switch for high-power energy storage applications," in *Proc. 2017 IEEE First Ukraine Conf. Elect. Comput. Eng.*, 2017, pp. 589–592.

[59] C. Bai, B. Han, and M. Kim, "A bidirectional switch based half-bridge series-resonant converter operating in DCM and CCM," in *Proc. 2020 IEEE Appl. Power Electron. Conf. Expo.*, 2020, pp. 2109–2115.

[60] Z. Miao, G. Sabui, A. Moradkhani Roshandeh, and Z. J. Shen, "Design and analysis of DC solid-state circuit breakers using SiC JFETs," *IEEE Trans. Emerg. Sel. Topics Power Electron.*, vol. 4, no. 3, pp. 863–873, Sep. 2016.

[61] Q. Lu et al., "Design and analysis of a 375V/5kA solid state dc circuit breaker based on IGCT," in *Proc. 2018 IEEE Int. Power Electron. Application Conf. Expo.*, 2018, pp. 1–5.

[62] Y. Kinoshita, T. Ichiryu, A. Suzuki, and H. Ishida, "100 a solid state circuit breaker using monolithic GaN bidirectional switch with two-step gate-discharging technique," in *Proc. 2020 IEEE Appl. Power Electron. Conf. Expo.*, 2020, pp. 652–657.

[63] M. R. Mohammadi and H. Farzanehfard, "Analysis of diode reverse recovery effect on the improvement of soft-switching range in zero-voltage-transition bidirectional converters," *IEEE Trans. Ind. Electron.*, vol. 62, no. 3, pp. 1471–1479, Mar. 2015.

[64] J.-H. Lee et al., "Auxiliary switch control of a bidirectional soft-switching DC/DC converter," *IEEE Trans. Power Electron.*, vol. 28, no. 12, pp. 5446–5457, Dec. 2013.

[65] C. S. Wong, Y. P. Chan, L. Cao, L. Wang, K. H. Loo, and M. C. Wong, "A single-stage dynamically compensated IPT converter with unity power factor and constant output voltage under varying coupling condition," *IEEE Trans. Power Electron.*, vol. 35, no. 10, pp. 10121–10136, Oct. 2020.

[66] T. Hafeez, M. Numan, A. Zia, H. A. Qureshi, and H. Farooq, "A study on the design and analysis of a bidirectional IPT system for EV wireless charging by using switch-controlled capacitor," in *Proc. 2022 Int. Conf. Emerg. Trends Elect., Control, Telecommun. Eng.*, 2022, pp. 1–6.

[67] A. Safaee, H. R. Karshenas, D. Yazdani, A. Bakhshai, and P. Jain, "A novel soft-switched bidirectional single-phase PWM AC chopper with a lossless active snubber circuit," in *Proc. 26th Annu. IEEE Appl. Power Electron. Conf. Expo.*, 2011, pp. 1106–1110.

[68] A. Safaee, D. Yazdani, A. Bakhshai, and P. K. Jain, "Multiblock soft-switched bidirectional ac–ac converter using a single loss-less active snubber block," *IEEE Trans. Power Electron.*, vol. 27, no. 5, pp. 2260–2272, May 2012.

[69] K. Sung, R. Iijima, S. Nishizawa, I. Norigoe, and H. Ohashi, "Experimental investigation of normally-on type bidirectional switch for indirect matrix converters," in *Proc. 2014 Int. Power Electron. Conf. (IPEC-Hiroshima 2014 - ECCE ASIA)*, 2014, pp. 117–122.

[70] J. Gálvez, X. Perpiñà, M. Vellvehí, D. Sánchez, X. Jordà, and J. Millán, "Computation method and comparison of semiconductor power losses within bidirectional switches (bds)," in *Proc. 2017 Spanish Conf. Electron Devices*, 2017, pp. 1–4.

[71] J. Huber and J. W. Kolar, "Monolithic bidirectional power transistors," *IEEE Power Electron. Mag.*, vol. 10, no. 1, pp. 28–38, Mar. 2023.

[72] J. W. Kolar, J. Huber, and D. Zhang, "Monolithic bi-directional switches-opening new horizons in power electronics," in *Proc. 19th Int. Conf. Silicon Carbide Related Mater.*, ETH Zurich, Power Electronic Systems Laboratory, 2022.

Guangyu Wang (Graduate Student Member, IEEE) was born in Hebei, China. He received the B.Eng. degree in electrical engineering from the Northeast Electric Power University, Jilin, China, in 2018, the M.Sc. degree in sustainable energy technology, in 2021, from the University of Liverpool, Liverpool, U.K., where he is currently working toward the doctorate in electrical and electronic engineering.

His research interests include control of dc/dc and dc/ac converter, three port photovoltaic energy storage inverter, and bidirectional switch.

Huiqing Wen (Senior Member, IEEE) received the B.S. and M.S. degrees in electrical engineering from Zhejiang University, Hangzhou, China, in 2002 and 2006, respectively, and the Ph.D. degree in electrical engineering from the Chinese Academy of Sciences, Beijing, China, in 2009.

From 2009 to 2010, he was an Electrical Engineer with the GE (China) Research and Development Center Company, Ltd., Shanghai, China. From 2010 to 2011, he was an Engineer with the China Coal Research Institute, Beijing, China. From 2011 to 2012, he was a Postdoctoral Fellow with the Masdar Institute of Science and Technology, Abu Dhabi, UAE. Since 2013, he has been with the Department of Electrical and Electronic Engineering, Xi'an Jiaotong-Liverpool University, Suzhou, China, where he is currently a Professor. He has authored or coauthored more than 50 peer-reviewed technical papers in leading journals. His research interests include renewable energy, electric vehicle, power electronics, microgrid, and power semiconductor devices.

Dr. Wen is a Fellow of the Institution of Engineering and Technology. He is the Associate Editor for *IEEE Access*, *International Journal of Photoenergy*, and *Journal of Power Electronics*.

Wen Liu (Senior Member, IEEE) received the B.S. degree in electronic information technology from Peking University, Beijing, China, in 2004, and the Ph.D. degree in electronic information technology from Nanyang Technological University, Singapore, in 2008.

She is a Senior Associate Professor with the School of Advanced Technology, Xi'an Jiaotong-Liverpool University, Suzhou, China. To date, she has supervised seven Ph.D. students and more than 20 master's students to completion. She has authored or coauthored more than 50 journal papers, more than 40 conference papers, and applied more than 20 patents. Her research interests include GaN power devices and their circuit integration.

Dr. Liu is currently the Chair of IEEE CASS-EDS Joint Chapter Suzhou, and the Deputy Director of the Youth Innovation Promotion Committee of the Third Generation Semiconductor Industry Technology Innovation Strategy Alliance (CASA), China.

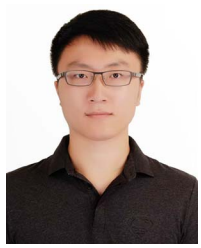

Fan Li (Member, IEEE) received the Ph.D. degree in electrical and electronic engineering from the University of Liverpool, Liverpool, U.K., and Xi'an Jiaotong-Liverpool University, Suzhou, China, in 2024.

His research interests include gallium nitride (GaN) power devices, monolithic integration, device modelling, and related advanced semiconductor technologies. He has contributed to several IEEE journals and conferences. He is actively engaged in the development of next-generation power electronics.